

Hund's metallicity and orbital-selective Mott localization of CrO₂ in the paramagnetic state

Mu-Yong Choi

Department of Physics, Myongji University, Yongin 17058, Korea

We present electronic structure calculations of a CrO₂ compound in the paramagnetic state within the computational scheme of density-functional theory combined with dynamical mean-field theory. We find that CrO₂ in the paramagnetic state is a strongly-correlated Hund's metal with mixed-valent Cr ions. At high temperatures, CrO₂ shows an orbital-selective Mott phase, in which the Cr d_{xy} orbital is Mott-localized while the other Cr t_{2g} d orbitals remain itinerant. When the temperature is lowered, the orbital-selective Mott state is found to evolve into a Kondo-like heavy-fermion state with a small pseudo gap at the Fermi level if the system remains in the paramagnetic state.

PACS numbers: 71.30.+h, 71.27.+a, 72.15.Qm, 71.20.Be

I. INTRODUCTION

Chromium dioxide (CrO₂) is a ferromagnetic metal with a Curie temperature of ~ 390 K.¹ Ferromagnetic CrO₂ exhibits half-metallic behavior with one of the two spin bands metallic and the other insulating.² Since fully spin-polarized metals can be very useful in spintronics applications, significant attention has been given to CrO₂,³ though the role of electron-electron interactions and the correlated electronic structure in CrO₂ have been embroiled in controversy and remains a subject of active research.^{4,5}

Electron-electron correlation is a key concept in understanding transition-metal oxides. A fascinating consequence of electron-electron correlation is the Mott metal-insulator transition in partially-filled bands, a proper explanation of which requires effort beyond the traditional single-electron approach to solids. A consistent theoretical framework for understanding of this phenomenon is provided via dynamical mean-field theory (DMFT).⁶ DMFT studies show that the Mott physics gets richer in multiband systems.⁷⁻¹⁴ A particular example is the orbital-selective Mott transition in partially filled multi-orbital systems, for which the Mott localization takes place in some orbitals, while the rest remains itinerant.^{7,8,11-15} The most obvious condition that can lead to an orbital-selective Mott transition is that orbitals have different intraorbital Coulomb repulsion.¹⁶ For systems having the same intraorbital Coulomb repulsion for all orbitals, degenerate correlated bands of different bandwidths^{7,8} or the crystal-field splitting of original degenerate bands^{11,12} has been identified as a prerequisite for the orbital-selective Mott transition. In either case, a sufficiently strong Hund's coupling is essential to develop the orbital-selective Mott phase (OSMP). The Hund's coupling or interorbital exchange may promote a strong differentiation of the correlation strength among the different orbitals which leads to the orbital-selective Mott localization. The idea of selective localization in the same subshell has recently received a great deal of attention.^{17,18}

In most compounds, the ratio of the local direct

Coulomb interaction to the bandwidth determines the strength of the correlations, while the Hund's coupling plays a subsidiary role. However, it has been shown¹⁹⁻²³ that in systems with multiple correlated bands crossing the Fermi level, the crucial role for strong correlation can be played by the Hund's coupling, rather than by the direct Coulomb interaction. The strength of electronic correlation in these systems is much more sensitive to the Hund's coupling than to the direct Coulomb interaction and therefore materials which exhibit this are often referred to as Hund's metals.^{23,24} Hund's metals in the paramagnetic state exhibit very large resistivity and Curie-Weiss-like magnetic susceptibility associated with well-formed local magnetic moments. This picture is significant for transition-metal oxides with partially-filled t_{2g} bands that are well separated from the empty e_g band by a crystal field. Some of iron-based high-temperature superconductors are a good example of Hund's metals.^{20,25,26} When a crystal field further lowers the symmetry and induces additional splitting in the original degenerate t_{2g} bands, the Hund's coupling may also develop the orbital-selective Mott localization in the transition-metal oxides.

CrO₂ forms a rutile structure with space group D_{4h}^{14} : $P4_2/mnm$. The unit cell contains two CrO₂ formula units. The Bravais lattice is tetragonal with lattice constants $a = b = 0.4421$ nm and $c = 0.2917$ nm.²⁷ The Cr atoms form a body-centered tetragonal lattice and are surrounded by octahedra of O atoms. The octahedra are slightly distorted away from the ideal geometry, with the apical O atoms slightly more distant from the central Cr atom than the equatorial O atoms. In the octahedral crystal field, the Cr $3d$ orbitals are split into a low-energy t_{2g} triplet and a high-energy e_g doublet. Distortion of the Cr-O octahedron further lifts the triple degeneracy of the t_{2g} orbitals, leading to three bands with predominantly xy and $yz \pm zx$ characters. If Cr is in its formal $4+$ valence state, the remaining two d electrons are expected to occupy the t_{2g} valence bands. Density-functional-theory (DFT) calculations^{2,28-31} show that the Cr t_{2g} orbitals are strongly hybridized with the O $2p$ orbitals to form dispersive bands crossing the Fermi level (EF). The O $2p$

bands also extend to EF and act as hole reservoirs, resulting in Cr being mixed valent.³¹ Measurements of the local magnetic susceptibility in the paramagnetic phase reveal a Curie-Weiss-like behavior with a local moment of $\sim 2\mu_B$.³ Resistivity measurements show that CrO₂ is a bad metal at high temperatures with the resistivity which exceeds the Mott limit.³² Both measurements demonstrate the possibility that the Cr *d* electrons are strongly correlated in the paramagnetic state. The local direct Coulomb interaction (*U*) and Hund's coupling (*J*) between *d* electrons, evaluated via constrain method, are as large as *U* = 3 eV and *J* = 0.87 eV.³¹ This indicates that both the Hund's coupling and the direct Coulomb-interaction between *d* electrons are quite strong for CrO₂. These characteristics make CrO₂ a strong candidate for a Hund's metal, with a possible OSMF in the paramagnetic state.

The density-functional theory combined with the dynamical mean-field theory (DFT+DMFT) is a powerful theoretical method for studying strongly-correlated materials beyond the limit of the standard density-functional theory.³³ The DFT+DMFT calculations of CrO₂ in the ferromagnetic state have been performed previously, showing the importance of dynamical correlation effects and the Hund's coupling in the material without considering the possibilities of Hund's metallicity and OSMF.^{34,35} In this paper, we present the electronic structure calculations of the CrO₂ compound in the paramagnetic state within the DFT+DMFT computational scheme, with a focus on the possibilities of Hund's metallicity and OSMF.

II. METHODS

The charge-self-consistent DFT+DMFT calculations are performed as presented in Ref. 36. The DFT part of the DFT+DMFT calculations is carried out employing the full-potential linearized augmented-plane-wave band method implemented in the WIEN2k package³⁷. The generalized gradient approximation with Perdew-Burke-Ernzerhof exchange-correlation functional³⁸ is adopted to describe the exchange and correlation potentials. A $8 \times 8 \times 13$ *k*-point grid is used for Brillouin-zone integrations. The continuous-time quantum Monte Carlo method^{39,40} is used as an impurity solver of the DMFT part to yield the local self-energy of the correlated *d* electrons. We include the Slater form of the Coulomb repulsion in its fully-rotationally-invariant form³⁶ to address the quantum impurity problem. The Slater integrals F^0 , F^2 , and F^4 are determined using the relations for *d* orbitals, $U = F^0$, $J = (F^2 + F^4)/14$, and $F^4/F^2 = 0.625$.⁴¹ The maximum entropy method⁴² is employed for analytical continuation of the local self-energy to the region of real frequencies.

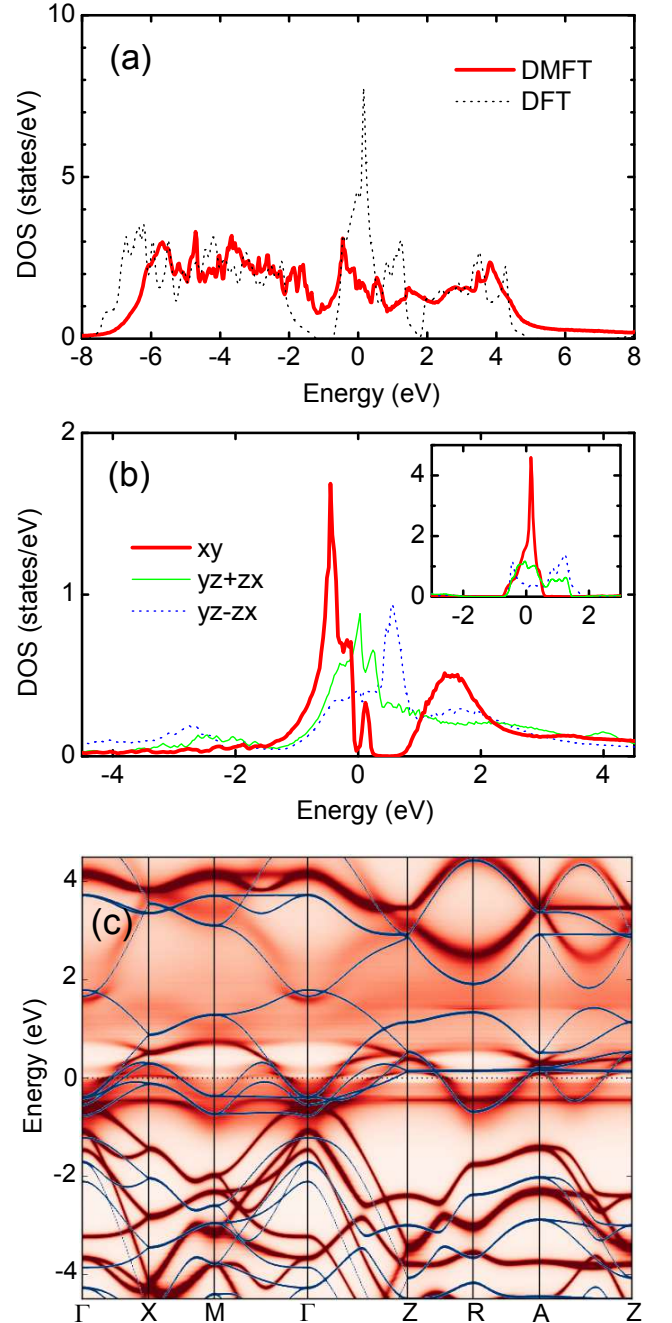


FIG. 1. (Color online) Band structure of CrO₂ in the paramagnetic state at 400 K obtained from the DFT+DMFT calculations with *U* = 3.0 eV and *J* = 0.9 eV. (a) Total density of states per formula unit, compared to the results of the DFT calculations. The dotted line denotes the corresponding DFT band structure. (b) Cr-*t*_{2g} orbital-resolved density of states. The inset shows the corresponding DFT band structure. (c) Momentum-resolved total spectral functions along high-symmetry lines in the Brillouin zone. The corresponding DFT bands are indicated as blue lines.

III. RESULTS AND DISCUSSION

We find from the DFT+DMFT calculations that Cr in this material is mixed valent, in agreement with the DFT calculations. The Cr valence is 2.4, smaller than expected from the ionic picture. Figure 1 illustrates the band structure of CrO_2 at 400 K obtained from the DFT+DMFT calculations. $U = 3.0$ eV and $J = 0.9$ eV are used in the calculations, as suggested by the *ab initio* calculations^{31,35} and previous experimental works⁵. The total density of states (total DOS) vs. energy plot in Fig. 1(a) demonstrates that a DMFT treatment of electron correlations induces significant modification in the band structure via DFT calculations. In comparison with the DFT bands, the low-energy bands of predominantly O $2p$ character below EF are pushed up by ~ 0.6 eV and the quasi-particle bands around EF, which are the Cr t_{2g} bands hybridized with the O $2p$ states, exhibit a reduced band width with the total-DOS peak shifted below EF. The Cr- t_{2g} orbital-resolved DOS of Fig. 1(b) reveals that the total-DOS peak observed below EF originates from the xy orbital. At EF, the xy band exhibits a pseudo band gap and the $yz + zx$ band has a DOS peak. Neither the band gap nor the DOS peak at EF can be identified in the DFT bands shown in the inset of Fig. 1(b), which suggests that they originate from the electron correlations. In Fig. 1(b), we also find broad local maxima of DOS in the region between 1 and 3 eV, which are missing in the DFT bands. The momentum-resolved total spectral functions along some high-symmetry lines in Fig. 1(c) prove that the broad DOS local maxima between 1 and 3 eV correspond to the upper Hubbard bands. Localized in real space, Hubbard bands appear as a blurred region in the momentum plot of spectral functions. The corresponding lower Hubbard bands are less clear in the plot, because it has a very small spectral weight distributed over a broad frequency region, as shown in Fig. 1(b). The momentum plot of spectral functions also reveals that the quasi-particle band near EF with prominent d_{xy} character is nearly dispersionless, and is strongly correlated with a large electron-scattering rate. The DFT+DMFT bands clearly indicate strong correlations among d electrons in this material.

One way of verifying the Hund metallicity is examining the dependence of the magnetic susceptibility on the Hund's coupling strength as discussed in Ref. 20. The local magnetic susceptibility can be evaluated from the spin-spin correlation function:

$$\chi_{loc} = \int_0^\beta \langle S_z(0)S_z(\tau) \rangle d\tau, \quad (1)$$

where S_z is the spin of the Cr atom and β is the inverse temperature.⁴³ In Fig. 2, we show the local spin susceptibilities of a Cr atom both with and without the Hund's coupling. With the Hund's coupling turned off, the susceptibility approximately obeys the Pauli law and the DOS (not shown) resembles that of the DFT bands, indicative of insignificant electron correlations in

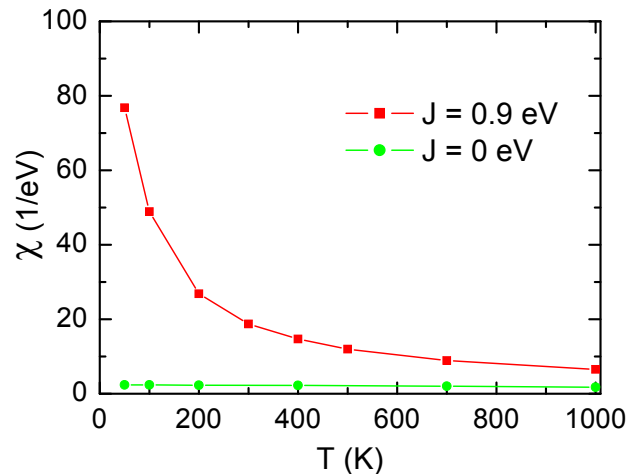


FIG. 2. (Color online) The local spin susceptibility of d electrons in a Cr atom as a function of temperature for different Hund's couplings, $J = 0$ and 0.9 eV.

the absence of the Hund's coupling. Doubling the direct Coulomb interaction brings marginal changes in the susceptibility and DOS. In contrast, when the Hund's coupling is turned on, the susceptibility becomes Curie-Weiss-like with a local moment of $\sim 1.5\mu_B$. The large local magnetic moment is a hallmark of strong correlations. The magnetic-susceptibility calculations indicate that with the Hund's coupling turned on, the system becomes a strongly-correlated metal retaining the local nature of magnetic moment. We thus conclude that CrO_2 is a Hund's metal, in which the strength of electron-electron correlation is almost entirely due to the Hund's coupling.

We now focus our attention on the orbital-resolved DOS to investigate the possibility of OSMP. Figure 3 displays the evolution of the Cr- t_{2g} orbital-resolved DOS with temperature.⁴⁴ At high temperatures, the xy orbital clearly exhibits a wide band gap at EF and the $yz \pm zx$ orbitals exhibit a finite DOS at EF, indicating that the strongly-correlated xy orbital is in an insulating state, while the other two orbitals are in itinerant states. The insulating gap of the xy orbital increases with enhanced U above 3 eV and disappears when U is lowered to 2 eV, as illustrated in Fig. 4. These behaviors are consistent with the system forming OSMP with the xy orbital in the Mott insulating state. As the temperature is lowered, the insulating gap of the xy orbital diminishes and is eventually superseded by a Kondo-like peak, as shown in Fig. 3. For the metallic $yz + zx$ orbital, the Kondo-like peak forms even at higher temperatures. When the temperature decreases below 100 K, the Kondo-like peak of the xy orbital splits to develop a small pseudo gap at EF. It has been shown⁴⁵⁻⁴⁷ that hybridization between orbitals can replace OSMP with a Kondo-like heavy-fermion regime at low temperatures. If the system actually enters into the Kondo-like heavy-fermion regime at low temperatures, two states are pos-

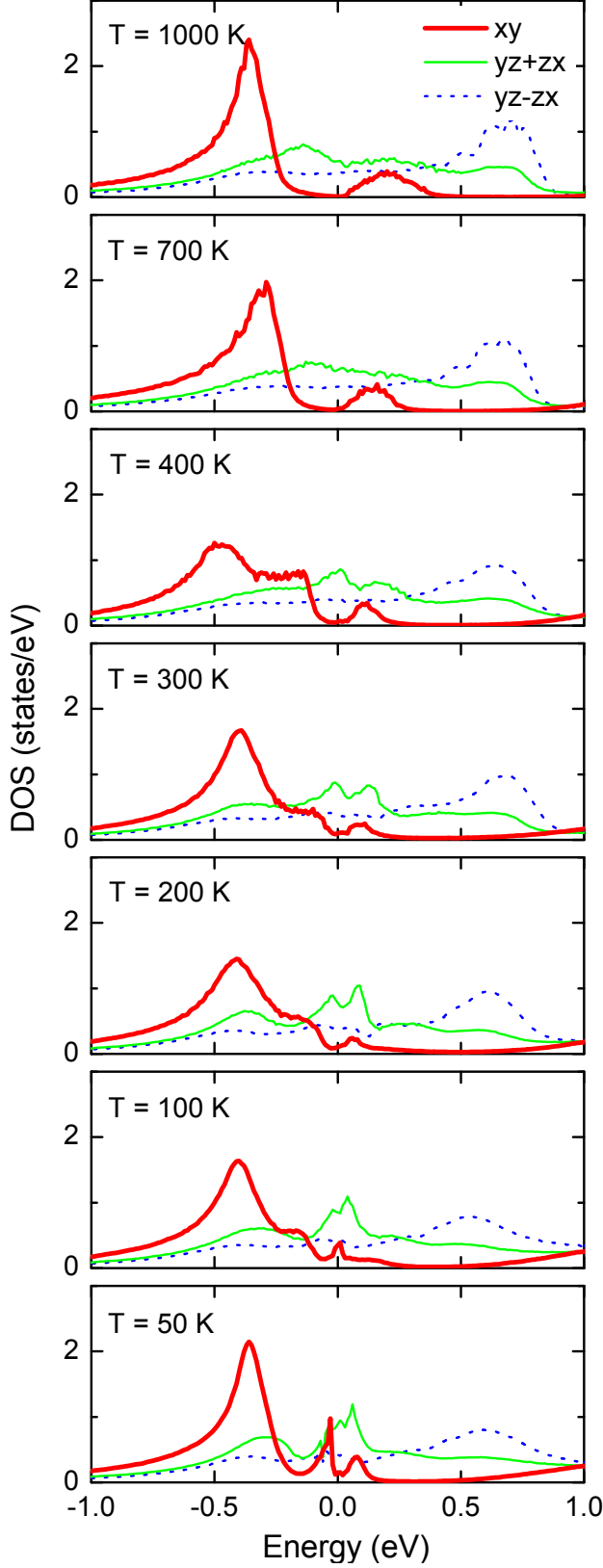


FIG. 3. (Color online) Evolution of the Cr- t_{2g} orbital-resolved density of states with temperature.

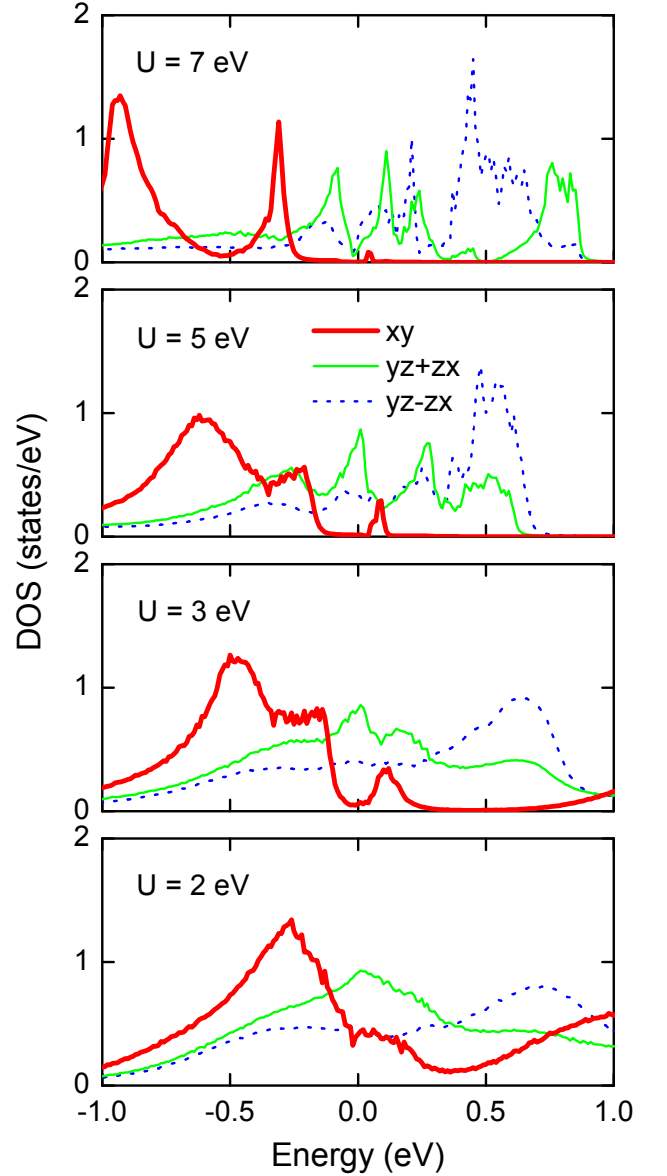


FIG. 4. (Color online) Cr- t_{2g} orbital-resolved density of states at 400 K for various U 's and the same $J/U = 0.3$.

sible, either a heavy-fermionic metallic state or a Kondo insulator with a small band gap between the bonding and antibonding bands. We would thus say that CrO₂ in a high-temperature OSMP is possibly driven by hybridization between d orbitals to a low-temperature Kondo-like metallic state which eventually acquires a Kondo insulating gap below 100 K, if the system remains in the paramagnetic state.

Most of the experimental studies on the electronic structure of CrO₂ have been carried out on ferromagnetic samples. Recent photoemission-spectroscopy measurements on ferromagnetic CrO₂ identifies the presence of the lower Hubbard band, indicating the correlated Mott-Hubbard-type electronic structure of this material.⁵ Ex-

perimental work on the electronic structure of paramagnetic CrO_2 , to the best of our knowledge, is limited to the temperature-dependent optical-conductivity measurements across the ferromagnetic transition presented in Ref. 48. The conductivity spectra display a Drude contribution at low frequencies, a broad peak in the mid-infrared region, and a sharp onset of interband absorption at ~ 1.5 eV demonstrating a distinct band gap. The main features of the spectra appear to be consistent with the DFT calculations for the ferromagnetic state showing EF lying in a band gap of the minority-spin DOS and crossing the majority-spin bands.^{2,28–31} However, the lack of temperature dependence of these features across the transition is in conflict with the DFT calculations, which predict the disappearance of the minority band gap and a drastically altered spectral-weight distribution for the paramagnetic state. Within the DFT scenario, the interband absorption above 1.5 eV is ascribed to interband transitions across the minority band gap.⁴⁸ The lack of temperature dependence of the sharp interband absorption above 1.5 eV implies the presence of a corresponding band gap on both sides of the ferromagnetic

transition. For the DFT+DMFT bands, it is tempting to assign the distinct absorption region above 1.5 eV to transitions from the quasi-particle bands near EF to the upper Hubbard bands which would stay put even below the Curie temperature. The experimental confirmation of OSMF for this material has yet to be made. Comprehensive photoemission-spectroscopy measurements above the Curie temperature should be a great help.

IV. CONCLUSIONS

To conclude, we find from DFT+DMFT calculations that CrO_2 in the paramagnetic state is a strongly-correlated Hund's metal. At high temperatures, CrO_2 shows an orbital-selective Mott phase in which the $\text{Cr } d_{xy}$ orbital is Mott localized, while the other t_{2g} d orbitals remain itinerant. With the temperature lowered, the orbital-selective Mott state is found to evolve into a Kondo-like heavy-fermion state with a small pseudo gap at EF if the system remains in the paramagnetic state.

-
- ¹ J. S. Kouvel and D. S. Rodbell, J. Appl. Phys. **38**, 979 (1967).
 - ² K. Schwarz, J. Phys. F **16**, L211 (1986).
 - ³ B. L. Chamberland, Critical Reviews in Solid State and Material Sciences **7**, 1 (1977).
 - ⁴ M. I. Katsnelson, V. Y. Irkhin, L. Chioncel, A. I. Liechtenstein, and R. A. De Groot, Rev. Mod. Phys. **80**, 315 (2008), and references therein.
 - ⁵ M. Sperlich, C. König, G. Güntherodt, A. Sekiyama, G. Funabashi, M. Tsunekawa, S. Imada, A. Shigemoto, K. Okada, A. Higashiya, M. Yabashi, K. Tamasaku, T. Ishikawa, V. Renken, T. Allmers, M. Donath, and S. Suga, Phys. Rev. B **87**, 235138 (2013), and references therein.
 - ⁶ A. Georges, G. Kotliar, W. Krauth, and M. J. Rozenberg, Rev. Mod. Phys. **68**, 13 (1996).
 - ⁷ V. I. Anisimov, I. A. Nekrasov, D. E. Kondakov, T. M. Rice, and M. Sigrist, Eur. Phys. J. B **25**, 191 (2002).
 - ⁸ A. Koga, N. Kawakami, T. M. Rice, and M. Sigrist, Phys. Rev. Lett. **92**, 216402 (2004).
 - ⁹ A. Liebsch, Phys. Rev. Lett. **91**, 226401 (2003).
 - ¹⁰ A. Liebsch and H. Ishida, Phys. Rev. Lett. **98**, 216403 (2007).
 - ¹¹ P. Werner and A. J. Millis, Phys. Rev. Lett. **99**, 126405 (2007).
 - ¹² L. de'Medici, S. R. Hassan, M. Capone, and X. Dai, Phys. Rev. Lett. **102**, 126401 (2009).
 - ¹³ T. Kita, T. Ohashi, and N. Kawakami, J. Phys.: Conf. Ser. **391**, 012157 (2012).
 - ¹⁴ E. Jakobi, N. Blümer, and P. van Dongen, Phys. Rev. B **87**, 205135 (2013).
 - ¹⁵ R. Yu and Q. Si, Phys. Rev. Lett. **110**, 146402 (2013).
 - ¹⁶ J. Wu, P. Phillips, and A. Castro Neto, Phys. Rev. Lett. **101**, 126401 (2008).
 - ¹⁷ M. Neupane, P. Richard, Z.-H. Pan, Y.-M. Xu, R. Jin, D. Mandrus, X. Dai, Z. Fang, Z. Wang, and H. Ding, Phys. Rev. Lett. **103**, 097001 (2009).
 - ¹⁸ M. Yi, D. H. Lu, R. Yu, S. C. Riggs, J.-H. Chu, B. Lv, Z. K. Liu, M. Lu, Y.-T. Cui, M. Hashimoto, S.-K. Mo, Z. Hussain, C. W. Chu, I. R. Fisher, Q. Si, and Z.-X. Shen, Phys. Rev. Lett. **110**, 067003 (2013).
 - ¹⁹ P. Werner, E. Gull, M. Troyer, and A. J. Millis, Phys. Rev. Lett. **101**, 166405 (2008).
 - ²⁰ K. Haule and G. Kotliar, New J. Phys. **11**, 025021 (2009).
 - ²¹ P. Hansmann, R. Arita, A. Toschi, S. Sakai, G. Sangiovanni, and K. Held, Phys. Rev. Lett. **104**, 197002 (2010).
 - ²² L. de'Medici, J. Mravlje, and A. Georges, Phys. Rev. Lett. **107**, 256401 (2011).
 - ²³ A. Georges, L. de'Medici, and J. Mravlje, Annual Reviews of Condensed Matter Physics **4**, 137 (2013).
 - ²⁴ Z. P. Yin, K. Haule, and G. Kotliar, Nat. Mater. **10**, 932 (2011).
 - ²⁵ F. Hardy, A. E. Bohmer, D. Aoki, P. Burger, T. Wolf, P. Schweiss, R. Heid, P. Adelmann, Y. X. Yao, G. Kotliar, J. Schmalian, and C. Meingast, Phys. Rev. Lett. **111**, 027002 (2013).
 - ²⁶ N. Lanata, H. U. R. Strand, G. Giovannetti, B. Hellsing, L. de'Medici, and M. Capone, Phys. Rev. B **87**, 045122 (2013).
 - ²⁷ P. Porta, M. Marezio, J. P. Remeika, and P. D. Dernier, Mat. Res. Bull. **7**, 157 (1972).
 - ²⁸ S. P. Lewis, P. B. Allen, and T. Sasaki, Phys. Rev. B **55**, 10253 (1997).
 - ²⁹ I. I. Mazin, D. J. Singh, and C. Ambrosch-Draxl, Phys. Rev. B **59**, 411 (1999).
 - ³⁰ A. Toropova, G. Kotliar, S. Y. Savrasov, and V. S. Oudovenko, Phys. Rev. B **71**, 172403 (2005).
 - ³¹ M. A. Korotin, V. I. Anisimov, D. I. Khomskii, and G. A. Sawatzky, Phys. Rev. Lett. **80**, 4305 (1998).

- ³² K. Suzuki and P. M. Tedrow, Phys. Rev. B **58**, 11597 (1998).
- ³³ G. Kotliar, S. Y. Savrasov, K. Haule, V. S. Oudovenko, O. Parcollet, and C. A. Marianetti, Rev. Mod. Phys. **78**, 865 (2006).
- ³⁴ L. Craco, M. S. Laad, and E. Müller-Hartmann, Phys. Rev. Lett. **90**, 237203 (2003).
- ³⁵ L. Chioncel, H. Allmaier, E. Arrigoni, A. Yamasaki, M. Daghofer, M. I. Katsnelson, and A. I. Lichtenstein, Phys. Rev. B **75**, 140406 (2007).
- ³⁶ K. Haule, C.-H. Yee, and K. Kim, Phys. Rev. B **81**, 195107 (2010).
- ³⁷ P. Blaha, K. Schwarz, G. K. H. Madsen, D. Kvasnicka, and J. Luitz, in *Wien2K*, edited by K. Schwarz (Technical Universität Wien, Austria, 2001).
- ³⁸ J. P. Perdew, K. Burke, and M. Ernzerhof, Phys. Rev. Lett. **77**, 3865 (1996).
- ³⁹ K. Haule, Phys. Rev. B **75**, 155113 (2007).
- ⁴⁰ E. Gull, A. J. Millis, A. I. Lichtenstein, A. N. Rubtsov, M. Troyer, and P. Werner, Rev. Mod. Phys. **83**, 349 (2011).
- ⁴¹ B. Himmetoglu, A. Floris, S. de Gironcoli, and M. Cococcioni, Int. J. Quantum Chem. **114**, 14 (2014).
- ⁴² M. Jarrell and J. E. Gubernatis, Phys. Rep. **269**, 133 (1996).
- ⁴³ In DMFT approximation, the local magnetic susceptibility is the local spin susceptibility of the impurity atom, which is somewhat different from the spin susceptibility of the lattice. Calculating the lattice spin susceptibility requires much more elaborate efforts, as discussed in Ref. 6.
- ⁴⁴ The orbital-resolved DOS at 400 K shown in Fig. 3 are slightly different from those in Fig. 1(b). The discrepancy results from different frequency increments used for the analytical continuation of the same self-energy to the region of real frequencies. For detailed illustration of DOS near EF, a reduced frequency increment is demanded as an input parameter for the analytical continuation. Such an input-parameter-dependent outcome is an intrinsic disadvantage of the maximum entropy method for analytical continuation.
- ⁴⁵ A. Koga, N. Kawakami, T. M. Rice, and M. Sigrist, Phys. Rev. B **72**, 045128 (2005).
- ⁴⁶ L. de'Medici, A. Georges, and S. Biermann, Phys. Rev. B **72**, 205124 (2005).
- ⁴⁷ E. A. Winograd and L. de'Medici, Phys. Rev. B **89**, 085127 (2014).
- ⁴⁸ M. K. Stewart, K. B. Chetry, B. Chapler, M. M. Qazilbash, A. A. Schafgans, A. Gupta, T. E. Tiwald, and D. N. Basov, Phys. Rev. B **79**, 144414 (2009).